PCCP

Cite this: *Phys. Chem. Chem. Phys.*, 2012, **14**, 6611–6616

www.rsc.org/pccp

PAPER

Tuning metal hydride thermodynamics *via* size and composition: Li–H, Mg–H, Al–H, and Mg–Al–H nanoclusters for hydrogen storage†

Lucas K. Wagner,[a] Eric H. Majzoub,[b] Mark D. Allendorf[c] and Jeffrey C. Grossman[d]

Received 20th December 2011, Accepted 14th March 2012
DOI: 10.1039/c2cp24063g

Nanoscale Li and intermetallic Al–Mg metal hydride clusters are investigated as a possible hydrogen storage material using the high-level quantum Monte Carlo computational method. Lower level methods such as density functional theory are qualitatively, not quantitatively accurate for the calculation of the enthalpy of absorption of H_2. At sizes around 1 nm, it is predicted that Al/Mg alloyed nanoparticles are stable relative to the pure compositions and the metal composition can be tuned in tandem with the size to tune the hydrogen absorption energy, making this a promising route to a rechargeable hydrogen storage material.

Introduction

Finding a portable fuel to replace petroleum poses an enormous challenge, since liquid gasoline is energy-dense, safe and easy to transport, and has an existing infrastructure. Batteries have much lower energy density and long charge times, and biofuel generation is still economically inefficient while potentially displacing valuable agricultural resources.[1] Using hydrogen as an energy carrier is very attractive, since it offers high energy density, can be generated cleanly from water,[2] and is used efficiently by fuel cells. However, since hydrogen at atmospheric pressure has a very low volumetric energy density, costly high pressure tanks must be used to achieve sufficient capacity for onboard vehicular storage.[3] Metal hydrides are attractive as vehicular hydrogen storage materials due to their high hydrogen content, thermodynamic stability relative to physisorption materials (which require cryogenic temperatures to achieve high hydrogen concentration), and ease of containment relative to high-pressure gas.[4] However, a major obstacle for most metal hydrides is insufficient equilibrium H_2 vapor pressure under conditions expected for fuel-cell operation. The desirable range of desorption enthalpies (ΔH°) is narrow, around 20–50 kJ mol^{-1},[4] to allow H_2 desorption at standard operating temperatures for a polymer electrolyte membrane fuel cell while remaining stable enough to be recharged at the H_2 pump.

The narrow range required for ΔH° lies roughly between two physical bounds: chemical bonds that are usually too strong, and hydrogen bonds that are usually too weak. Combined with the strict weight requirements, it is a challenge to find a bulk material with ideal physical properties. One promising strategy to address this problem is to utilize the surface energy of materials at the nanoscale as an additional lever to adjust ΔH°. Nanoscale hydride materials have been successfully synthesized.[5–7] $NaAlH_4$ in particular has been found to be stabilized at the nanoscale relative to decomposition of the hydrogen both in experiment[8] and in theory,[9,10] and also to have faster desorption kinetics,[10–12] $LiBH_4$ has also been considered, showing improved kinetics[13] and predicted destabilization at the nanoscale.[14] However, MgH_2 is destabilized by less than 10 kJ mol^{-1} H_2 except at the extremely small scale,[15–20] not enough to put it in the 20–50 kJ mol^{-1} range. The origin of the observed effects remains an open question, since it is difficult to experimentally distinguish kinetic effects from changes in thermodynamics, while theoretical calculations based on density functional theory (DFT) may not be able to predict ΔH° to the accuracy required, as noted by Wu *et al.* and Wolverton *et al.* for clusters of MgH_2,[15,16] having errors of 15–20 kJ mol^{-1} H_2 compared to experiment or high level quantum simulation. Nanoscale hydrogen storage is thus very promising, but it still remains a great challenge to understand the behavior of ΔH° to a sufficient level to design a practical hydrogen storage system.

In this article, we use high accuracy fixed node diffusion quantum Monte Carlo (DMC) calculations to evaluate the change in energy in the reaction $(MH_m)_n \rightarrow M_n + \frac{m}{2}H_2$ for several different metal atoms M (Li, Mg, Al, and two alloys of MgAl). Our objective is to help resolve two major questions: first to what extent we can use size and composition to control the hydrogen desorption energy ΔH° of metal hydride materials, and second, how much we can rely on DFT to carry out computational

[a] *Department of Physics, University of Illinois at Urbana-Champaign, USA. E-mail: lkwagner@illinois.edu*
[b] *Center for Nanoscience, and Department of Physics and Astronomy, University of Missouri-St. Louis, USA*
[c] *Sandia National Labs, Livermore*
[d] *Department of Materials Science and Engineering, Massachusetts Institute of Technology, USA. E-mail: jcg@mit.edu*

† Electronic supplementary information (ESI) available: Geometries and energetics of all the nanoclusters considered in this paper. See DOI: 10.1039/c2cp24063g

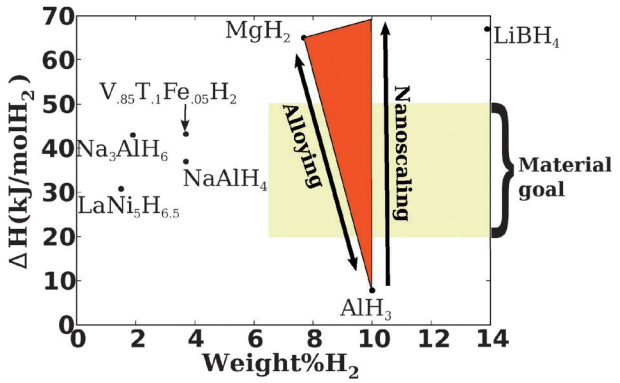

Fig. 1 Hydrogen storage material parameters attainable by combining nanoscale effects and alloying. By performing both, we are able to access values of the hydrogen desorption entropy that are unattainable in bulk for stability reasons. Several bulk materials are given; material parameters are taken from Yang *et al.*[4]

materials design for hydrogen storage. Our motivation for the specific choice of metals in this study is as follows. First, both Li and Mg have a small number of valence electrons, enabling benchmarking of our methods using high accuracy quantum chemistry calculations. Second, the bulk MgH_2 and AlH_3 stoichiometries provide two extremes with respect to hydride stability: MgH_2 is too stable, making its use in fuel-cell vehicles unfeasible. On the other hand, AlH_3 is too unstable, making onboard regeneration unfeasible. In this study, we have found that mixed Mg–Al nanoclusters are predicted to have intermediate stability and that their size/composition can be tuned to obtain H_2 desorption thermodynamics within the desired range for onboard hydrogen storage, as summarized in Fig. 1.

Approach

To summarize the computational scheme, DMC calculations were benchmarked for small clusters using the quantum chemistry technique CCSD(T) and for the bulk limit where experimental data are available to verify accuracy. Minimum energy structures of metal hydride and pure metal clusters were generated with the number of metal atoms up to 20, and hydrogen desorption energies ΔE are evaluated using both DFT and DMC. This is expected to be a very good approximation to the change in enthalpy ΔH° since standard pressure is very small compared to the internal energy in these nanostructures.

The most challenging aspect of these calculations is locating the lowest energy structure of small nanoparticles. In general, this is an exponentially scaling problem, although in practice the clusters do adopt the crystalline structure once the number of metal atoms is large enough. Our interest, however, is in the $\sim$1 nm regime, where most atoms reside at the surface, and the cluster is quite different from bulk. Representative geometries are pictured in Fig. 2.

For the molecular systems, we used NWChem[21] with a cc-pTZP[22] basis set to evaluate all density functional theory energetics. Diffusion Monte Carlo calculations were performed using QWalk[23] at the B3LYP[24] minimum energy geometry. Using the PBE or other density functionals to find the geometry did not change the DMC energetics. The orbitals were generated using the GAMESS[25] package and used in a Slater-Jastrow wave function in the QWalk[23] package. For Li, cusp corrections were introduced into the basis set for the nuclei, and the Jastrow factor was the two-body one given in ref. 23. We used the modified Green's function given in ref. 26 to obtain a small timestep error converged at 0.01 Hartrees^{-1}.

For the coupled cluster calculations, we have used the Tensor Contraction Engine[27] in NWChem. To obtain complete basis set estimates, we have used the extrapolation function $E(n) = E_{CBS} + \alpha/n^4$, since that extrapolation gave the smallest change between $n = 3,4$ and $n = 4,5$ extrapolations.

For the solid Li and LiH, we used Crystal2003[28] to generate PBE[29] orbitals for DMC. We averaged over a $2 \times 2 \times 2$ k-point grid for twisted average boundary conditions.[30] We then fit to a $1/N_{atom}$ dependence and extrapolated to remove the finite size corrections. Stochastic errors are given by the Bayesian technique in ref. 31.

We evaluated the correction to the energy due to thermal motions and zero-point energy (ZPE) motion of the nuclei in DFT(PBE) using the harmonic approximation. For most of the calculations here, we leave it out in order to compare total energies. Since the ZPE correction is rather small compared to the differences between theoretical approaches, we account for the ZPE only when comparing to experimental numbers.

The minimum energy structures for the stoichiometric LiH nanoclusters can be found by simply constructing rectangular prisms that contain an equal number of Li and H atoms, as used by Manby *et al.*[32] in a different context. We confirmed using the Prototype Electrostatic Ground State(PEGS)[33] searches that these structures are in fact the minimum energy states. For the other hydrides, we used only the PEGS[33] geometries. Briefly, the PEGS method utilizes a Wang-Landau Monte Carlo algorithm and simple electrostatic Hamiltonian to rapidly search the potential energy surface of ionic compounds and produce prototype structures for further refinement with density functional theory. This now well-established method successfully finds the correct ground-state structures for bulk ionic complex hydrides[34–38] and has been extended with the use of Wang-Landau Monte Carlo to obtain minimum energy geometries for ionic nanoclusters.[9] This extensive search increases the likelihood that the structures subsequently used in the DMC and DFT calculations represent the lowest energy for the sizes considered and increases the validity of comparisons with experimental data.

The minimum energy geometries for the pure metal nanoclusters are not accurately reproduced using a simple electrostatic potential and thus require other methods. Fournier and others[39] performed a search for Li, but to our knowledge, structures for other metal compositions are unknown. The geometry calculations were performed as following:

1. Generate an atom at the origin.
2. Loop from 1 to $n - 1$.

(a) Choose an atom currently existing in the cluster.

(b) Generate a new atom by choosing a random direction and placing it one bond length away.

3. If no atoms are within a cutoff radius of each other, continue with the calculation. Otherwise, return to 1.
4. Optimize the geometry of the configuration with respect to the DFT(PBE) energy.

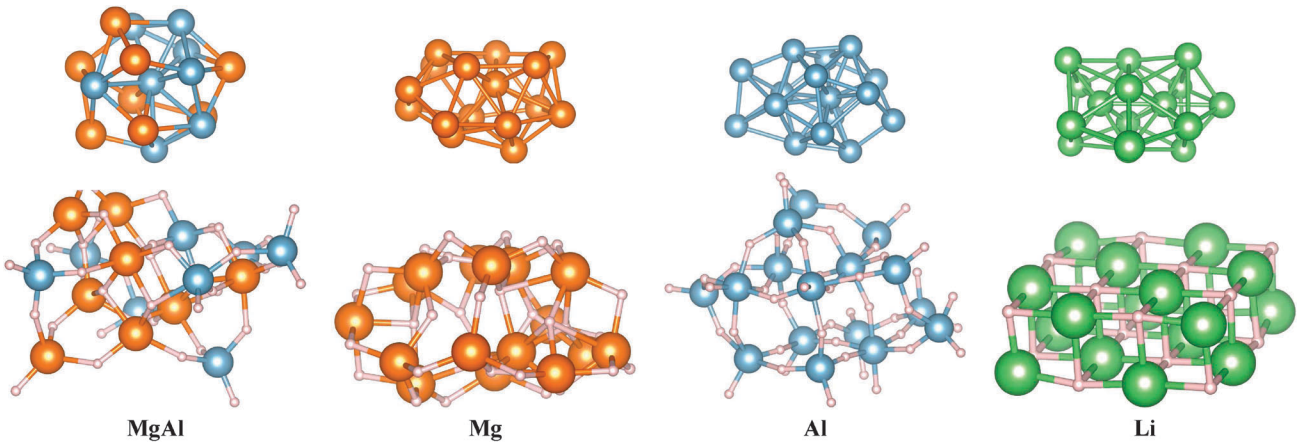

Fig. 2 Representative structures of the clusters found using the search method discussed in the text. The metal atoms are larger, with Al darker than Mg.

5. After 50 trial configurations are generated and optimized, stop and determine the lowest energy.

We include the geometries we used as well as their energies in the supplementary information.† We tested using up to 200 trial configurations on the cluster Mg_9Al_9 and found that the energy had converged to within about 0.5 kJ mol^{-1} H_2, well within the energy changes considered in this work. This method is similar in concept to the random structure search used by Pickard and Needs.[40] Although this algorithm is quite simple, it is able to reproduce all the clusters found in previous work,[39] and we cross-checked this algorithm against the PEGS method for hydrides, both finding the same lowest energy structures. We also verified for several compositions that using DFT(PBE)-selected minimum energy structures instead of using DMC-selected minimum energy structures did not change the reaction energy.

Table 1 Desorption energy (kJ mol^{-1}) benchmarks of DMC performance. Where reference zero point energy data was available, we corrected the reference data for zero point energy, marked with †; the others have the DMC data corrected using PBE estimations of the zero point energy. The CCSD(T) value marked with a * was performed with a smaller extrapolation of triples and quadruples, the rest with quadruples and quintuples

	DMC	CCSD(T)	Exp
$LiH \rightleftharpoons Li + \frac{1}{2} H_2$ †	22.7(6)	22.70	
$(LiH)_2 \rightleftharpoons 2Li + H_2$ †	134.5(6)	129.18	
Bulk Li †	199.9(6)		181(2)[32,41]
$(MgH_2)_1 \rightleftharpoons Mg + H_2$	−13.4	−13.6	
$(MgH_2)_2 \rightleftharpoons 2Mg + 2H_2$	46.8	49.1	
Mg bulk	77.5(5)[16]		75
$AlH_3 \rightleftharpoons Al + \frac{3}{2} H_2$ †	142.0	137.9*	
α Al bulk	11(1)		9.9(6)[42]

Results and discussion

In Table 1, DMC results are compared with highly accurate extrapolated CCSD(T)[27] calculations for clusters for which it was feasible to converge the CCSD(T) basis. On the other end of the size spectrum, the DMC results are compared to experiment. DMC obtains near chemical accuracy for the hydrogen desorption energy (around 4–8 kJ mol^{-1}) for all the reference values we calculated, with the only exception being bulk LiH, which has a small error due to an underestimation of the cohesive energy of Li metal.

Confident that our DMC results are near chemical accuracy for hydrogen desorption energies, we next use this approach to evaluate the cluster energies in the intermediate region between bulk and the very small clusters. This is an area where the DMC method is particularly useful, since no other method can calculate energies to the same level of accuracy on clusters of this size. In this section, we evaluate the accuracy of several common DFT functionals for this problem, summarized in Fig. 3. To aid in the comparison, we do not correct these energies for zero point energy and thus report them as the quantity ΔE, the change in electronic energy. Note that curves for the Mg/MgH_2 clusters are smoother than in Wu *et al.*[16] because the cluster geometries used in the earlier work did not always correspond to the lowest energy structures for each particle size. We see that the commonly used density functional theories have errors on the order of ±20 kJ mol^{-1} H_2 compared to the DMC data.

The low performance of DFT can be understood by a simple analysis of the bonding patterns of the metallic and hydride clusters. Generally speaking, the hydride nanoparticles have ionic character, in which the hydrogen acts as a charge acceptor (see Fig. 4 in which most of the charge density is localized around the hydrogens), while bonding in the pure-metal clusters becomes increasingly metallic as the cluster size increases. Evaluating the difference between these two qualitatively different states is a challenging problem for any electronic structure method, since both must be described to equal accuracy. Since the localization of both the ionic and metallic clusters changes at different rates as the number of atoms changes, the error in DFT functionals considered here also changes as a function of the number atoms. For example, in this case, it appears that the hybrid functionals M06 and B3LYP, despite including some portion of Hartree–Fock exchange to reduce the self-interaction error, are not significantly more accurate than LDA and PBE. The scaling behavior of ΔE for such systems is therefore of use in benchmarking new density functionals. To that end, we have included raw data in the supplemental information, sufficient to reproduce our results.†

Another route to predict the scaling of energies with size is to use the Wulff construction, as for example has been employed by Kim and coworkers for binary hydrides,[43] who provided

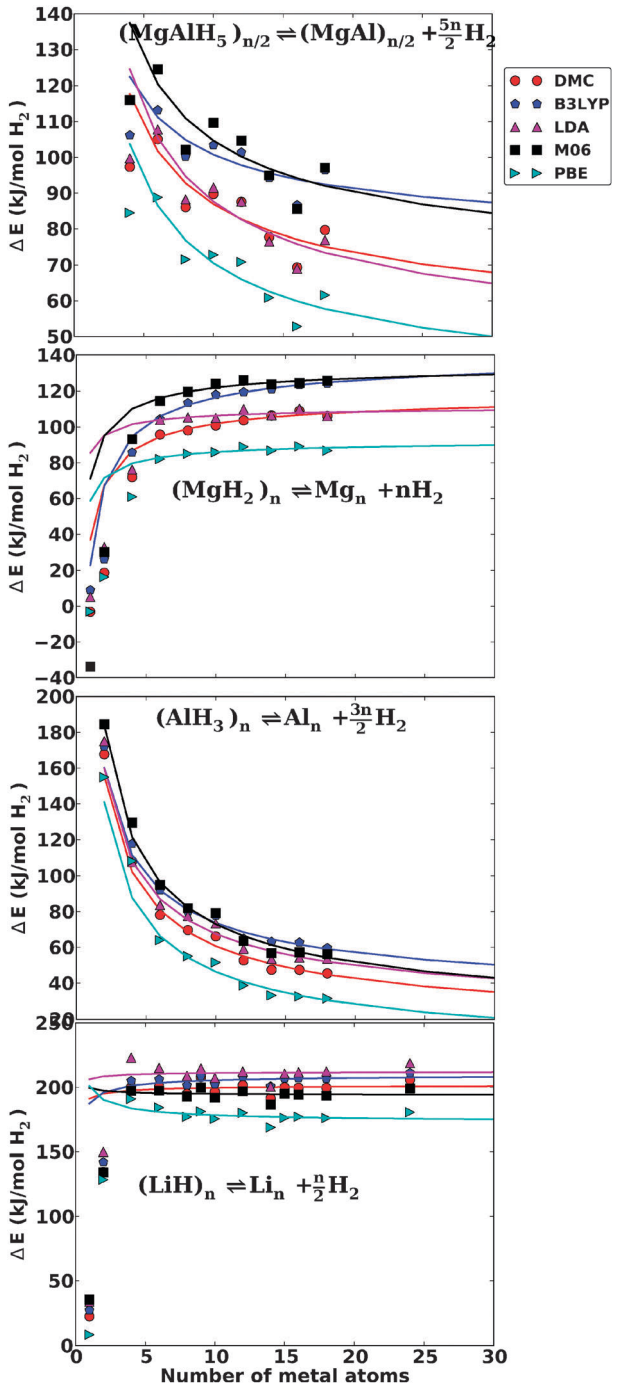

Fig. 3 The trends of the reaction energy for various methods, along with fits to $\Delta E(n) = \alpha/n^{2/3} + \beta$ (solid lines). The stochastic errors of the DMC data are smaller than the symbol sizes. The CCSD(T) results are indistinguishable from the DMC results on these scales.

scaling data for ΔE proportional to $n^{-2/3}$, with n the number of metal atoms. This method uses the surface energies of the bulk crystal to construct a minimum energy nanocrystal, and has been applied to many simple metal hydrides using DFT(PW-91) energetics for the surface energies. There are two major concerns with this approach: first with the accuracy of the DFT energetics themselves, and second with the applicability of the mesoscale Wulff construction to predict effects at the nanoscale. We can test both of these using our data.

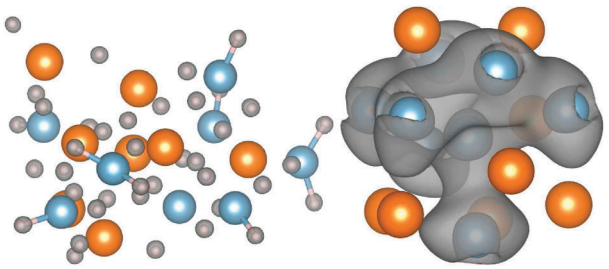

Fig. 4 The valence electron density isosurfaces at 50% maximum for Mg_8Al_8 and $Mg_8Al_8H_{40}$ clusters. Note that the density is diffuse for the metallic cluster while it is highly ionic for the hydride cluster. Colors are the same as in Fig. 2.

Our results are compared to the Wulff construction by fitting our data to $\alpha n^{-2/3} + \beta$, with α and β being fitting parameters. The resulting parameters are summarized in Table 2 and the fits are shown compared to the calculated data in Fig. 3. The fits for Li and Al appear to be quite good, reproducing the bulk limits without explicit fitting, while Mg has an anomaly also seen by others,[16,20] in which it attains a maximum around 15 metal atoms, which is due to the formation of a bulk-like core in the hydride around that size.[17] This anomaly does not affect the following analysis, since the Wulff construction cannot replicate this effect and pure Mg hydride clusters are too strongly bound to be a hydrogen storage material, even at the nanoscale. The DFT α calculated for the nanoclusters (see Fig. 3) are generally qualitatively correct compared to the DMC, while the results of the Wulff construction (Table 2) are substantially different, which shows that the Wulff construction is not accurate at these very small sizes, as noted by Kim *et al.*[43] This is due to the fact that at these ~1 nm sizes, the nanoparticles are too far from their crystalline form for the Wulff construction to be applicable. Since most of the changes in ΔE occur at small nanoparticle sizes, a bottom-up approach is more amenable to this problem.

For nanoscale metal hydrides to be used for hydrogen storage, one must be able to sufficiently control the size to achieve the

Table 2 The fitted parameters for $n > 5$ in kJ mol^{-1} H_2, in the equation $\Delta E(n) = \alpha/n^{2/3} + \beta$, where n is the number of metal atoms. The size range in which the particles are estimated to lie in the 20–50 kJ mol^{-1} hydrogen desorption energy is also listed. Mg and Li are not included in the latter because they can never achieve the 20–50 kJ mol^{-1} range

Name	DMC	B3LYP	LDA	M06	PBE	Wulff[43]
			α			
Mg	−83(8)	−119(9)	−27(3)	−65(9)	−35(4)	−29
MgAl	170(22)	119(15)	204(18)	181(27)	183(17)	N/A
$MgAl_2$	234(21)					
Al	229(15)	209(3)	223(20)	268(10)	228(14)	10
Li	−11(8)	−23(8)	−6(12)	6(6)	29(9)	79
			β			
Mg	120(2)	142(2)	112(1)	136(2)	93(1)	
MgAl	50(4)	75(3)	44(4)	66(5)	31(4)	
$MgAl_2$	28(6)					
Al	11(3)	29(1)	20(4)	15(2)	−3(3)	
Li	202(1)	210(1)	212(2)	194(1)	172(2)	
Estimated size range with ΔE in the range 20–50 kJ mol^{-1}						
MgAl	74-bulk	Never	44-bulk	Never	16-bulk	
$MgAl_2$	20–1150					
Al	10–40	17–2000	13–100	15–80	7–20	

desired desorption energy of 20–50 kJ mol^{-1}. The predicted size ranges in which the hydrogen desorption energy falls in this range are listed in Table 2. Here we can see the effect of the errors of DFT as manifested in the size range predictions; the estimated ranges are dramatically different for different functionals. These predictions are very sensitive to the scaling behavior, so the accuracy of the methods used is critical. From the DMC results, note that the estimated size range for the MgAl alloy is from around 74 metal atoms up to the bulk, whereas Al alone has only a very small range between 10 and 40 atoms. This confirms that alloying can significantly alter the size range in which nanoparticles have the desired desorption energies.

To check our conjecture that alloying interpolates between the two base metals, we test the $MgAl_2/MgAl_2H_8$ stoichiometry in addition to the $MgAl/MgAlH_5$ stoichiometry, shown in Table 2. Since we were not interested in using this system as a benchmark, we did not evaluate all the DFT functionals for this composition. Our calculations show that the alloys interpolate well between the pure materials, which can be understood from the fact that the hydrides are ionic (observed already for LiH[44] and responsible for the effectiveness of the PEGS method[33]) and the pure metallic clusters have metallic bonding. Therefore, there are no bond networks to create nonlinear effects as a function of size. There are only magic numbers in the binding energy of the metals for small sizes, but this effect diminishes with increasing size and does not change the overall trend.

For the most part, the alloys are stabilized by nanoscale effects (Fig. 5). This effect has also been noted in other calculations, for example in an Au–Pt[45] alloy and for several III–V nanomaterials.[46] We thus would not expect such an alloy to spontaneously segregate, although it is possible that some other composition would be more stable. It seems likely that a hypothetically more stable composition would also have a ΔE (and thus ΔH°) somewhere between the two non-alloyed states, because of the additive behavior mentioned above. We can thus envision a tunable hydrogen storage system that uses alloys of Mg and Al. Either the alloy composition or particle size can be tuned to optimize the ease of making and storing the nanoparticles, while the other variable can be tuned to obtain the correct desorption energy. Kinetics at the nanoscale will likely be much improved over the bulk systems.[10–12]

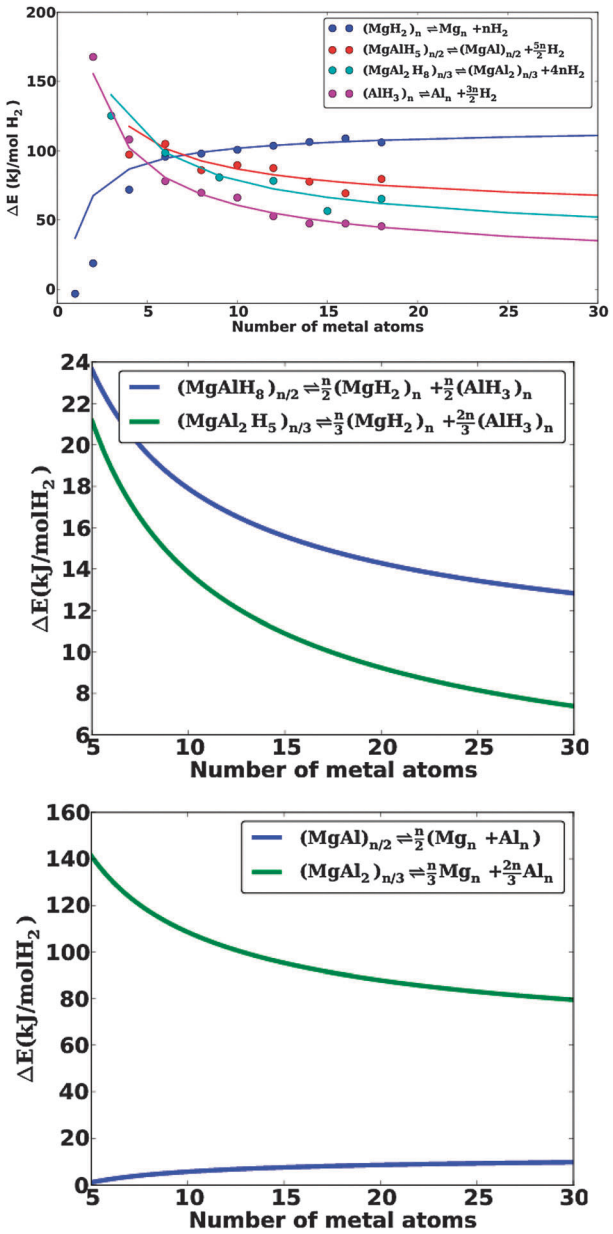

Fig. 5 Stability of the alloy hydride and metallic clusters to decomposition into single-element particles. Only the fits to $1/n^{2/3}$ are shown here.

Conclusion

To summarize, we have performed high accuracy calculations of the hydrogen desorption energies (ΔE) of small metallic nanoclusters using diffusion quantum Monte Carlo (DMC) techniques and minimum energy structures. We find a strong size dependence in the scaling of ΔE as the nanoparticle size becomes close to 1 nm. Comparing the results to density functional theory (DFT), the error in ΔE is approximately $\pm$20 kJ mol^{-1} H_2, while the target range is 20–50 kJ mol^{-1} H_2. This error is large enough to incorrectly predict the ideal size of nanoparticle that hits the target ΔE for on-board storage applications, and Wulff models based on bulk surface energies also differ substantially from the DMC results. We thus suggest that future calculations use DMC energetics to correct the DFT ones; the computational cost is not prohibitive, about the same as the relaxation of the atomic coordinates in DFT. Our results show that alloys of Mg and Al are stabilized at the nanoscale and that ΔE can be tuned to intermediate regimes between the strongly bound MgH_2 and weakly bound AlH_3. Alloying metal hydrides at the nanoscale is thus a promising method for controlling the hydrogen desorption thermodynamics of these materials, and could potentially form the basis of a new hydrogen storage system.

Acknowledgements

Thanks to Kevin Rasch for providing input files for solid Li. This work was supported by the U.S. Department of Energy Office of Hydrogen, Fuel Cells, and Infrastructure Program. We also thank NSF Teragrid for computational resources.

References

1 J. Fargione, J. Hill, D. Tilman, S. Polasky and P. Hawthorne, *Science*, 2008, **319**, 1235.
2 T. Bak, J. Nowotny, M. Rekas and C. Sorrell, *International Journal of Hydrogen Energy*, 2002, **27**, 991–1022.
3 L. Schlapbach and A. Zuttel, *Nature*, 2001, **414**, 353–8.
4 J. Yang, A. Sudik and C. Wolverton, *Chemical Society Reviews*, 2010, **39**, 656–675.
5 P. Ngene, P. Adelhelm, A. Beale, K. deJong and P. E. J. deJongh, *Phys. Chem. C*, 2010, **114**, 6163.
6 K.-F. Aguey-Zinsou and J.-R. Ares-Fernández, *Chem. of Mat.*, 2008, **20**, 376–378.
7 W. Lohstroh, A. Roth, H. Hahn and M. Fichtner, *Chem-PhysChem*, 2010, **11**, 789.
8 J. Gao, P. Adelhelm, M. H. W. Verkuijlen, M. Rongeat, C. Herrich, P. J. M. van Bentum, O. Gutfleisch, A. P. M. Kentgens, K. P. de Jong and P. E. J. de Jongh, *Phys. Chem. C*, 2010, **114**, 4675.
9 E. Majzoub, F. Zhou and V. Ozolins, *J. Phys. Chem. C*, 2011, **115**, 2636.
10 T. Mueller and G. Ceder, *ACS Nano*, 2010, **4**, 5647–5656.
11 N. Bazzanella, R. Checchetto and A. Miotello, *J. Nanomaterials*, 2011, **2011**, 1–11.
12 T. K. Nielsen, U. Bösenberg, R. Gosalawit, M. Dornheim, Y. Cerenius, F. Besenbacher and T. R. Jensen, *ACS Nano*, 2010, **4**, 3903–3908.
13 A. Gross, J. Vajo, S. VanAtta and G. Olson, *J. Phys.Chem. C*, 2008, **112**, 5651.
14 X. Liu, D. Peaslee, C. Z. Jost, T. F. Baumann and E. H. Majzoub, *Chem. Mater.*, 2011, **23**, 1331–1336.
15 C. Wolverton, D. J. Siegel, A. R. Akbarzadeh and V. Ozolins, *J. Phys.: Condens. Matter*, 2008, **20**, 064228.
16 Z. Wu, M. D. Allendorf and J. C. Grossman, *J. Am. Chem. Soc.*, 2009, **131**, 13918–13919.
17 S. Harder, J. Spielmann, J. Intemann and H. Bandmann, *Angew. Chem., Int. Ed.*, 2011, **50**, 4156–4160.
18 Z. Zhao-Karger, J. Hu, A. Roth, D. Wang, C. Kubel, W. Lohstroh and M. Fichtner, *Chem. Commun.*, 2010, **46**, 8353–8355.
19 M. Paskevicius, D. A. Sheppard and C. E. Buckley, *J. Am. Chem. Soc.*, 2010, **132**, 5077–5083.
20 R. W. P. Wagemans, J. H. van Lenthe, P. E. de Jongh, A. J. van Dillen and K. P. de Jong, *J. Am. Chem. Soc.*, 2005, **127**, 16675–16680.
21 M. Valiev, E. Bylaska, N. Govind, K. Kowalski, T. Straatsma, H. V. Dam, D. Wang, J. Nieplocha, E. Apra, T. Windus and W. de Jong, *Comput. Phys. Commun.*, 2010, **181**, 1477–1489.
22 J. Thom H. Dunning, *J. Chem. Phys.*, 1989, **90**, 1007–1023.
23 L. K. Wagner, M. Bajdich and L. Mitas, *J. Comput. Phys.*, 2009, **228**, 3390–3404.
24 P. J. Stephens, F. J. Devlin, C. F. Chabalowski and M. J. Frisch, *J. Phys. Chem.*, 1994, **98**, 11623–11627.
25 M. W. Schmidt, K. K. Baldridge, J. A. Boatz, S. T. Elbert, M. S. Gordon, J. H. Jensen, S. Koseki, N. Matsunaga, K. A. Nguyen, S. J. Su, T. L. Windus, M. Dupuis and J. A. Montgomery, *J. Comput. Chem.*, 1993, **14**, 1347.
26 C. J. Umrigar, M. P. Nightingale and K. J. Runge, *J. Chem. Phys.*, 1993, **99**, 2865–2890.
27 S. Hirata, *J. Phys. Chem. A*, 2003, **107**, 9887.
28 R. D. V. R. Saunders, C. Roetti, R. Orlando, C. M. Zicovich-Wilson, N. Harrison, K. Doll, B. Civalleri, I. Bush, P. DArco and M. Llunell, *CRYSTAL2003 User's Manual*, University of Torino, 2003.
29 J. P. Perdew, K. Burke and M. Ernzerhof, *Phys. Rev. Lett.*, 1996, **77**, 3865–3868.
30 C. Lin, F. H. Zong and D. M. Ceperley, *Phys. Rev. E: Stat. Phys., Plasmas, Fluids, Relat. Interdiscip. Top.*, 2001, **64**, 016702.
31 L. K. Wagner and L. Mitas, *J. Chem. Phys.*, 2007, **126**, 034105.
32 F. R. Manby, D. Alfe and M. J. Gillan, *Phys. Chem. Chem. Phys.*, 2006, **8**, 5178–5180.
33 E. H. Majzoub and V. Ozolincedilscaron, *Phys. Rev. B: Condens. Matter Mater. Phys.*, 2008, **77**, 104115.
34 Y. Zhang, E. Majzoub, V. Ozolins and C. Wolverton, *Phys. Rev. B: Condens. Matter Mater. Phys.*, 2010, **82**, 174107.
35 M. Anstey, M. Corbett, E. Majzoub and J. Cordaro, *Inorg. Chem.*, 2010, **49**(18), 8197.
36 E. Majzoub and E. Ronnebro, *J. Phys. Chem. C*, 2009, **113**, 3352–3358.
37 V. Ozolins, E. Majzoub and C. Wolverton, *J. Am. Chem. Soc.*, 2009, **131**, 230–237.
38 V. Ozolins, E. Majzoub and C. Wolverton, *Phys. Rev. Lett.*, 2008, **100**, 135501.
39 R. Fournier, J. B. Y. Cheng and A. Wong, *J. Chem. Phys.*, 2003, **119**, 9444.
40 C. Pickard and R. Needs, *Phys. Rev. Lett.*, 2006, **97**, 45504.
41 J. D. Cox, D. D. Wagman and V. A. Medvedev, *CODATA Key Values for Thermodynamics*, Hemisphere Publishing Corp., New York, 1989.
42 J. Graetz and J. J. Reilly, *J. Alloys Compd.*, 2006, **424**, 262–265.
43 K. C. Kim, B. Dai, J. K. Johnson and D. S. Sholl, *Nanotechnology*, 2009, **20**, 204001.
44 P. Fuentealba and A. Savin, *J. Phys. Chem. A*, 2001, **105**, 11531–11533.
45 S. Xiao, W. Hu, W. Luo, Y. Wu, X. Li and H. Deng, *Eur. Phys. J. B*, 2006, **54**, 479–484.
46 G. Guisbiers, M. Wautelet and L. Buchaillot, *Phys. Rev. B: Condens. Matter Mater. Phys.*, 2009, **79**, 155426.

